NACA RM E54D02

NACA

RESEARCH MEMORANDUM

EFFECT OF NOZZLE CONTOUR ON DRAG OF PARABOLIC AFTERBODIES

By Donald J. Vargo and Gerald W. Englert

Lewis Flight Propulsion Laboratory
Cleveland, Ohio

NATIONAL ADVISORY COMMITTEE
FOR AERONAUTICS

WASHINGTON
June 21, 1954
Declassified July 22, 1959

NATIONAL ADVISORY COMMITTEE FOR AERONAUTICS

RESEARCH MEMORANDUM

EFFECT OF NOZZLE CONTOUR ON DRAG OF PARABOLIC AFTERBODIES

By Donald J. Vargo and Gerald W. Englert

NASA

SUMMARY

The effect of nozzle internal contour on afterbody drag was investigated in the Lewis 8- by 6-foot supersonic wind tunnel. Five different nozzle-afterbody configurations were evaluated.

In general, for the same ratio of nozzle-exit area to throat area, changing the nozzle contour so that the angle between the axis of symmetry and the nozzle wall at the exit was increased caused an increase in the interaction of the exhaust jet on the afterbody drag. This interaction was such that, for the convergent-divergent nozzle configurations at low pressure ratios, the flow from the nozzles aspirated the base region and increased the drag. At high pressure ratios the jet interaction decreased the total external afterbody drag of both the convergent and convergent-divergent nozzles.

INTRODUCTION

Maximizing the thrust minus drag of jet-powered aircraft and missile configurations necessitates the selection of the most efficient exit nozzle and afterbody combination. Comparison of the different convergent-divergent nozzles presented in reference 1 shows a dependence of the nozzle thrust characteristics on the nozzle contour. The data of reference 1 also show, at low nozzle pressure ratios, a dependence of thrust or internal-flow results on external flow. Interaction effects between internal and external flow are further demonstrated in references 2 and 3, in which the drag of afterbodies is shown to be quite dependent on the jet issuing from the nozzle.

The investigation reported in reference 3 was to illustrate the effect of nozzle expansion ratio on jet afterbody interaction. Of equal interest is the influence at a given expansion ratio of the nozzle contour on afterbody drag.

This report presents the results of investigating the effect of three different convergent-divergent nozzle contours and two convergent

contours on the drag of surrounding parabolic afterbodies. These five nozzles were operated over a range of pressure ratios from jet-off to greater than 12 at free-stream Mach numbers of 1.6 and 2.0. The Reynolds number based on model length and free-stream flow conditions varied from 2.14×10^7 to 3.24×10^7.

SYMBOLS

The following symbols are used in this report:

C_D	drag coefficient based on maximum body area
C_p	pressure coefficient, $(p-p_0)/q_0$
k	constant in nozzle contour equation = $V_*^2 - V_1^2$
L	length of convergent portion of nozzle
M	Mach number
P	total pressure, lb/sq ft
P_1/p_0	nozzle pressure ratio
p	static pressure, lb/sq ft
q	dynamic pressure, $\gamma pM^2/2$, lb/sq ft
R	radius, in.
V	velocity, ft/sec
x	axial distance, in.
γ	ratio of specific heats

Subscripts:

a	boattail
b	base
N	nozzle
p	pressure
t	total

0	free stream
1	nozzle entrance
*	nozzle throat

APPARATUS AND PROCEDURE

The basic apparatus employed was a body of revolution supported in the Lewis 8- by 6-foot supersonic-wind-tunnel test section by means of two hollow struts (fig. 1(a)). The body consisted of a parabolic nose, a cylindrical centerbody, and the afterbody and exit-nozzle configuration being evaluated. The hollow support struts served the additional purpose of ducting high-pressure air into the model. After entering the model this internal air was turned 90°, passed through a honeycomb flow straightener, and then discharged through the test nozzle. In order to avoid the possible formation of condensation shocks in the nozzle, the air was preheated to 400° F.

The basic body had a maximum diameter of 8.25 inches and, for all nozzle configurations except the convergent-divergent uniform-exit type, was 83.75 inches long including the afterbody. This nozzle necessitated extension of the model length to 85.75 inches. The body was so mounted that the rear portion of the afterbody and part of the jet could be viewed from schlieren windows mounted in the tunnel walls.

A strain-gage type balance was located within the forebody of the model. With one side of the balance fixed or grounded to the support struts, the entire outer fairing of the basic body was attached to the free or measuring side of the balance (fig. 1(b)). Balance-derived drag forces were compared with forces obtained by an integration of static pressures supplied by pressure instrumentation on various sections of the model. A more detailed analysis of the body dimensions and force-reduction techniques employed is presented in the appendix of reference 4.

Two of the convergent-divergent nozzles used in this investigation utilized a basic convergent section that also served as one of the convergent nozzles. The contour of this section (fig. 2(b)), based on a one-dimensional flow analysis, was such that the acceleration of the air as a function of axial distance from the nozzle entrance to the throat followed the trignometric function $\frac{k}{L}\left(1 - \cos\frac{2\pi x}{L}\right)$, where L is the length of the convergent section and k equals the nozzle throat velocity squared minus the entrance velocity squared. This criterion yields a smooth bellmouth type of nozzle with quite uniform flow at

the throat. One of these convergent-divergent nozzles using the convergent section had a divergent portion (fig. 2(c)) that was expanded quite rapidly in an attempt to induce separation when the nozzle was only slightly overexpanded. The angle between the axis of symmetry and the wall of this nozzle at the exit station was 18.4°. The other convergent-divergent nozzle having this same convergent section also had a divergent section designed for uniform exit flow by use of axially symmetric characteristics (fig. 2(e)). This nozzle should, therefore, have a high efficiency at the design point.

The other convergent nozzle (fig. 2(a)) consisted of a 12°-half-angle cone. The remaining convergent-divergent nozzle (fig. 2(d)) consisted of a 25° conical convergent section attached to a 3.6° conical diverging section with a smooth fairing at the throat. This nozzle was geometrically similar to one of the nozzles reported in reference 5 in quiescent air. It had a ratio of exit to throat area of 1.39. The other two convergent-divergent nozzles had expansion area ratios of 1.44.

Two different boattails were used to encompass the five different nozzles. This was a result of the difference in exit diameters between the convergent and convergent-divergent nozzles, which in turn was due to fixing the throat diameter of all five nozzles at one value. The same equation (fig. 2), however, describes both boattails, that for the convergent-divergent nozzles being cut off shorter than the boattail for the convergent nozzles. A clearance of 0.1 inch between the boattail inner surface and nozzle outer wall was maintained for all nozzle configurations except the conical convergent-divergent type. For this case, the clearance was enlarged to approximately 0.2 inch, as the exit diameter of this nozzle was slightly less than that of the rapidly diverging and uniform-exit convergent-divergent nozzles.

The pressure ratio across the nozzle, which is defined as the total pressure at the nozzle entrance divided by the static free-stream pressure, was in most cases varied from approximately 12 to a jet-off condition. Data were obtained at free-stream Mach numbers of 2.0 and 1.6 and at zero angle of attack. Pressure orifices were located along the top, bottom, and side boattail surfaces, as is illustrated in figure 3. Base pressure was measured by means of three pressure tubes in the annulus between the boattail and nozzle walls.

RESULTS AND DISCUSSION

The flow issuing from the rear of an aerodynamic body will entrain air from the semidead base regions and thus tend to lower the pressure and increase the drag of the afterbody (ref. 2). Counteracting the drag increases due to this aspiration effect is a compression of the external flow by the interaction of the jet issuing from the nozzle.

This occurs because the external flow along the boattail of an aerodynamic body must in most cases make an abrupt change in direction when it meets the jet stream. When the free stream is supersonic, this abrupt change in direction is accompanied by the formation of an oblique shock. Because of the presence of the boundary layer on the boattail surface, the pressure increase across the shock may be transmitted upstream, thickening the boundary layer and replacing the original shock with a series of weaker shocks that fan out along the afterbody surface. As the pressure ratio across the nozzle is increased to the extent that the nozzle is underexpanded - that is, the exit static pressure of the nozzle is greater than the external ambient static pressure - the jet continues to expand or diverge after it leaves the nozzle exit. This additional divergence of the jet increases the strength of the previously mentioned shock waves and causes them to move forward, which movement tends to reduce the afterbody wave drag. This phenomenon has been demonstrated in references 2 and 3.

In addition to jet pressure ratio, a change in the nozzle contour can also increase jet divergence and result in external-flow changes similar to those just discussed. Differences in the stream shock pattern caused by change of nozzle contour are apparent in the schlieren photographs of figure 4. The sketch in the upper left hand corner is a composite of the main points of interest of the three photographs. These schlieren photographs were taken at a free-stream Mach number of 1.6 and at a nozzle pressure ratio (total pressure at nozzle entrance to free-stream static pressure) of 8.9. The position of shock coalescence about the afterbody fairing was the most rearward for the uniform-exit convergent-divergent nozzle. On the other hand, the oblique shock generated in the free stream attained the maximum position forward of the plane of the nozzle exit with the rapidly divergent nozzle. The variation of shock position was consistent with the variation of the angle between the axis of symmetry and the nozzle wall at the exit station; that is, an increasing angle drives the shock farther forward on the afterbody.

Boattail Pressure Drag

The boattail pressure drag obtained by integration of the pressures measured along the boattail surface $C_{D,a}$ is presented in figure 5 as a function of nozzle pressure ratio P_1/p_0. Since the conical convergent-divergent nozzle had an expansion area ratio (1.39) slightly different from that of the other two divergent nozzles (1.44), an additional variable is present in these drag curves (fig. 5(a)). Linear interpolation of data of reference 3 was used to attempt an adjustment of this data to an area ratio of 1.44. The results are shown by the dashed lines on the drag figures.

Some aspiration effect is indicated for the convergent-divergent nozzles at a free-stream Mach number M_0 of 1.6 and low pressure ratios, as the drag increases with an increase of pressure ratio. Beyond a pressure ratio of 6, which corresponds quite closely to the design pressure ratio of these nozzles, the aspiration effect is overshadowed by the previously discussed compression effects of the diverging jet on the external flow. This is demonstrated by a decrease of drag with an increase of nozzle pressure ratio.

Since the pressure ratio that the nozzle experiences (total pressure ahead of nozzle divided by static pressure at nozzle-exit station) is dependent on the flow about the afterbody, the correct P_1/p_0 corresponding to the design expansion ratio is a variable. If there were no external flow and no jet interference on the afterbody, the design pressure ratios for a ratio of specific heats of 1.4 and nonviscous flow would be 5.30 for the conical convergent-divergent nozzle and 5.75 for the remaining two convergent-divergent nozzles.

In general, the rapidly divergent nozzle had the highest drag of the three divergent nozzles at low pressure ratios (aspiration region) and the lowest drag in the underexpanded region (high-pressure-ratio region). The drag of the uniform-exit nozzle was the lowest of the three divergent nozzles in the low-pressure-ratio region and as high as or higher than the others in the high-pressure region.

No aspiration effect is indicated for the convergent nozzles presented in figure 5(b), probably because these nozzles were in an underexpanded condition over nearly all the range of pressure ratios studied; that is, the ratio of the total pressure of the nozzle entrance to the static pressure at the exit was nearly always greater than 1.89, assuming no entropy decrease. The compression or shock-interference effects are, therefore, quite pronounced, especially for the uniform-exit nozzle.

In general, increasing the nozzle-wall exit angle (considered positive when diverging) resulted in an increase in the boattail drag of the convergent-divergent nozzles at pressure ratios below design and a decrease in the boattail drag of both the convergent and convergent-divergent nozzle configurations at pressure ratios above design. Also, the trends of boattail drag with wall exit angle were more pronounced at free-stream Mach number of 1.6 than at 2.0.

Base Drag

The effect of changing nozzle contour on base pressure is presented in figure 6. In general, the base pressure was affected by the change

in nozzle contour in the same manner as was the boattail pressure. At low pressure ratios, increasing the nozzle-exit flow angle increased the drag of the convergent-divergent nozzle configurations. At high pressure ratios, increasing the exit angle decreased the drag of both the convergent and convergent-divergent nozzle configurations. As was the case for boattail pressures, the effect of nozzle pressure ratio P_1/p_0 on the base pressure was greater at a free-stream Mach number of 1.6 than at 2.0.

In general, the base pressure for a given nozzle pressure ratio is higher at a free-stream Mach number of 1.6 than at 2.0, which is in agreement with reference 6. Some of this increase of base pressure with decrease of free-stream Mach number may possibly be due to strut shocks reflected from the tunnel walls (fig. 4) passing approximately one jet diameter downstream of the model-exit station (ref. 7). This effect is believed to be quite small, however, because of the small wake region following the base of this model (base diameter/jet diameter of approximately 1.1).

Total Drag

The total drag of the model measured with the strain-gage balance system is shown in figure 7. Since the forebody and centerbody of this model do not vary with internal-flow conditions or nozzle geometry, these curves are representative of trends of the jet influence on afterbody drag. Since the influence of the jet on friction drag of the boattail is small (ref. 3), these curves have the same general characteristics as the boattail and base pressure drag curves.

A comparison of the results obtained from the balance system with those obtained by calculation and pressure integration is shown in figure 8. Forebody pressure drag computed by the method of reference 8, total friction drag obtained from reference 3, and base drag computed from figure 6 were subtracted from total drag obtained from the balance system. The results of above calculation (dashed curves) were compared with the boattail pressure drag obtained from figure 5. In general, the resulting trends of boattail pressure drag with nozzle contour, free-stream Mach number, and jet pressure ratio were the same for both types of measurement; however, the calculated values were slightly higher than those derived from pressure integration.

A change in contour of a convergent-divergent nozzle, while holding the design expansion ratio constant, may result in either loss or gain of thrust due to changes in the radial component of momentum, friction losses, internal shock losses, and separation characteristics of the nozzle (refs. 1, 5, and 9). As a rule, the afterbody drag is rather small

3257

compared with the magnitude of the jet thrust. The thrust minus drag of the afterbody and nozzle configuration may, therefore, have entirely different trends from the drag results presented herein. It appears, however, that for the case of convergent nozzles and over the range of pressure ratios studied herein the thrust minus drag of the nozzle and afterbody configuration can be improved by changing from a conical nozzle to one of uniform-exit or bellmouth design, as drag would be decreased and thrust would be at least as good as or better than before.

SUMMARY OF RESULTS

The effect of changes in nozzle contour of two convergent and three convergent-divergent nozzles on the drag of parabolic afterbodies was investigated over a range of pressure ratios from jet-off to greater than 12 at free-stream Mach numbers of 1.6 and 2.0. For this range of variables the following conclusions were reached:

1. Changing nozzle contour so that the angle between the axis of symmetry and the nozzle wall at the exit station (considered positive when diverging) was increased caused an increase in the total afterbody drag at low pressure ratios for the convergent-divergent nozzles. A decrease in afterbody drag, however, for both convergent and convergent-divergent nozzles was experienced with increase of exit angle at high pressure ratios.

2. Boattail drag and base drag exhibited the same general trends with nozzle contour, jet pressure ratio, and free-stream Mach number as total afterbody drag.

3. The influence of the jet on the afterbody was generally more pronounced at a free-stream Mach number of 1.6 than at 2.0.

Lewis Flight Propulsion Laboratory
National Advisory Committee for Aeronautics
Cleveland, Ohio, March 26, 1954.

REFERENCES

1. Fradenburgh, Evan A., Gorton, Gerald C., and Beke, Andrew: Thrust Characteristics of a Series of Convergent-Divergent Exhaust Nozzles at Subsonic and Supersonic Flight Speeds. NACA RM E53L23, 1954.

2. Cortright, Edgar M., Jr., and Schroeder, Albert H.: Investigation at Mach Number 1.91 of Side and Base Pressure Distributions over Conical Boattails Without and With Jet Flow Issuing from Base. NACA RM E51F26, 1951.

3. Englert, Gerald W., Vargo, Donald J., and Cubbison, Robert W.: Effect of Jet-Nozzle-Expansion Ratio on Drag of Parabolic Afterbodies. NACA RM E54B12, 1954.

4. Hearth, Donald P., and Gorton, Gerald C.: Investigation of Thrust and Drag Characteristics of a Plug-Type Exhaust Nozzle. NACA RM E53L16, 1954.

5. Krull, H. George, and Steffen, Fred W.: Performance Characteristics of One Convergent and Three Convergent-Divergent Nozzles. NACA RM E52H12, 1952.

6. Cortright, Edgar M., Jr., and Kochendorfer, Fred D.: Jet Effects on Flow over Afterbodies in Supersonic Stream. NACA RM E53H25, 1953.

7. Faro, I. D. V.: Experimental Determination of Base Pressures at Supersonic Velocities. Bumblebee Rep. No. 106, Appl. Sci. Lab., Johns Hopkins Univ., Nov. 1949. (Contract NOrd 7386, Bur. Ordnance, U. S. Navy.)

8. Jones, Robert T., and Margolis, Kenneth: Flow over a Slender Body of Revolution at Supersonic Velocities. NACA TN 1081, 1946.

9. Foster, Charles R., and Cowles, Frederick B.: Experimental Study of the Divergence-Angle Effect in Rocket-Motor Exhaust Nozzles. Prog. Rep. No. 20-134, Jet Prop. Lab., C.I.T., Jan. 16, 1951. (Contract DA 04-495-ORD 18.)

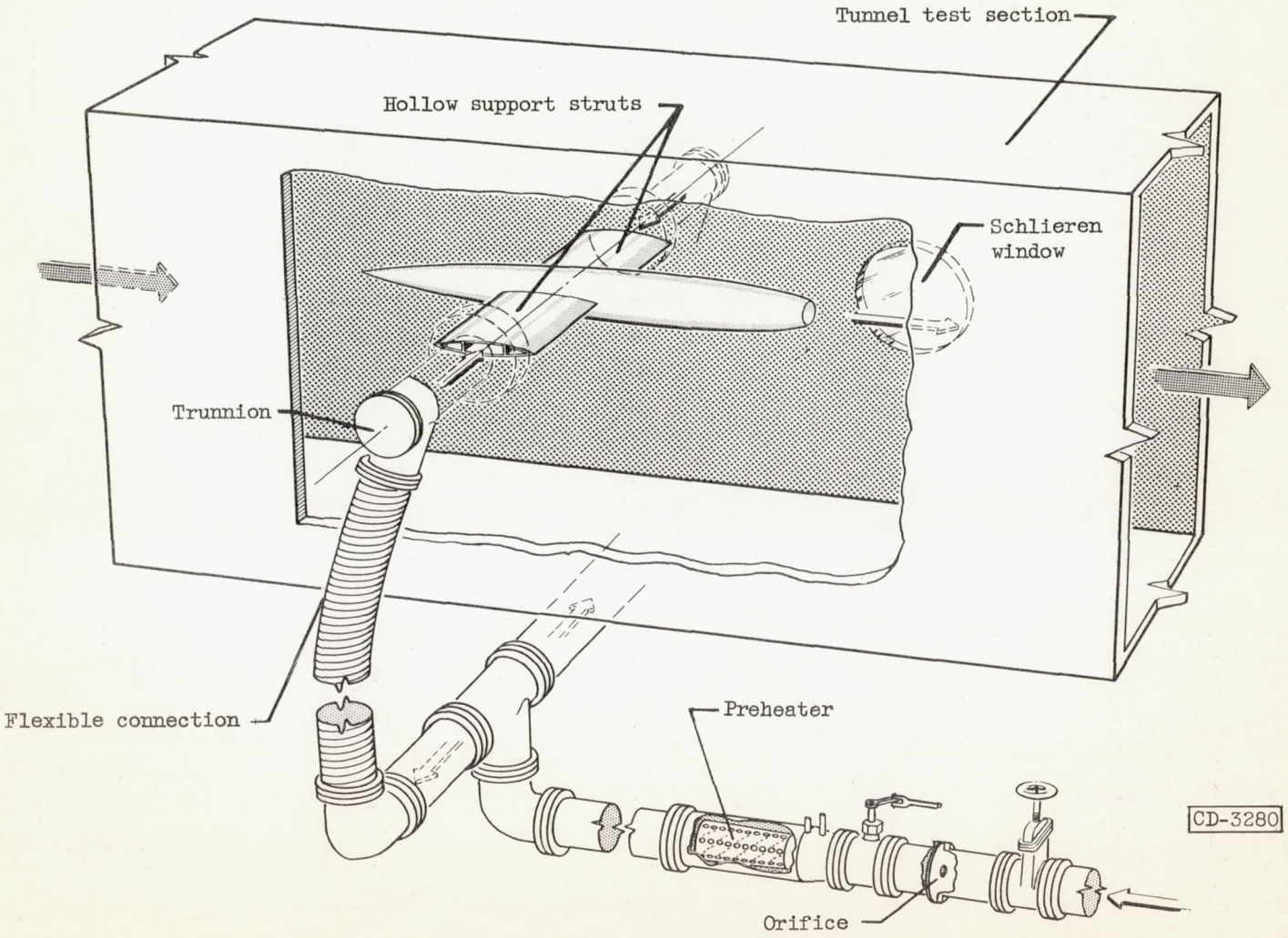

(a) Schematic drawing of jet-exit model in 8- by 6-foot supersonic-wind-tunnel test section.

Figure 1. - Experimental apparatus.

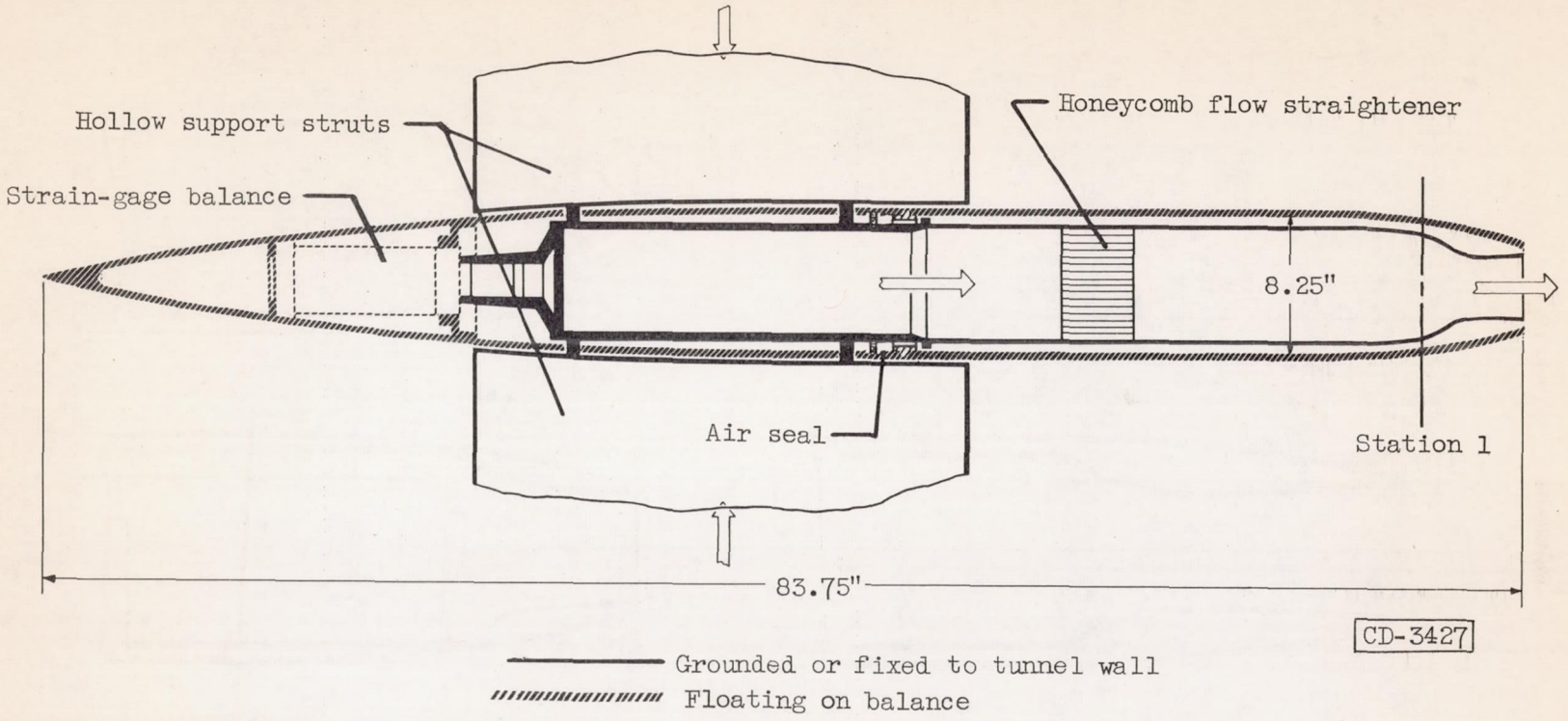

(b) Cross section of model.

Figure 1. - Concluded. Experimental apparatus.

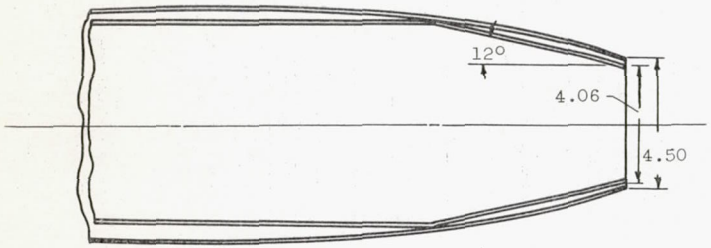

(a) Conical convergent.

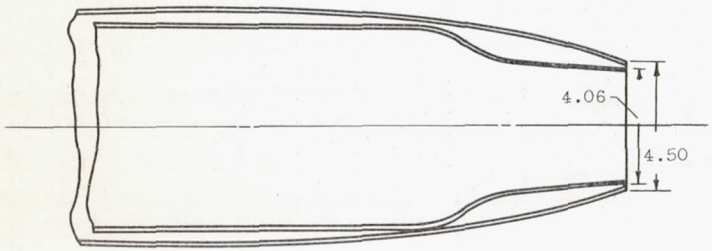

(b) Uniform-exit convergent.

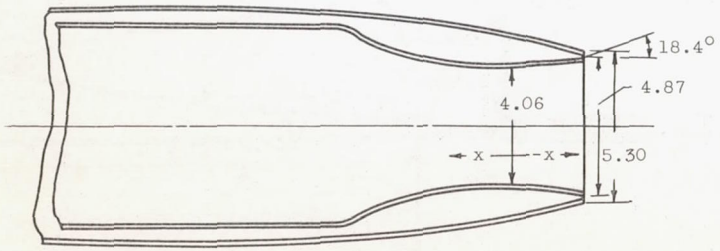

(c) Rapidly divergent. Design expansion ratio, 1.44.

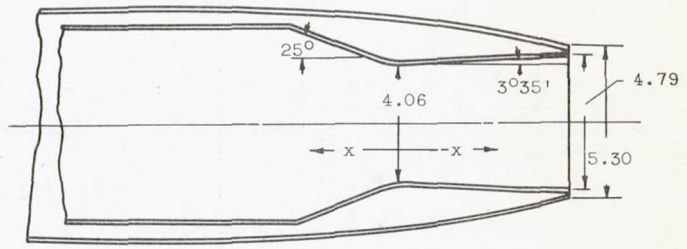

(d) Conical convergent-divergent. Design expansion ratio, 1.39.

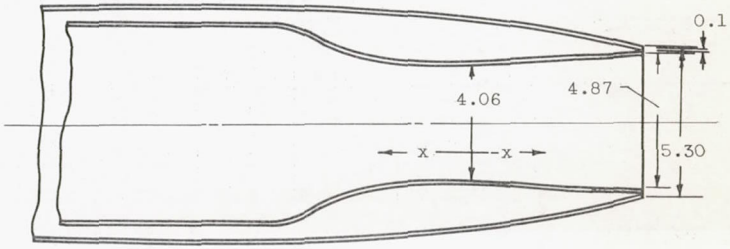

(e) Uniform-exit convergent-divergent. Design expansion ratio, 1.44.

Common convergent-section nozzles b,c,e		Divergent-section nozzle c		Divergent-section nozzle e	
x_N	R_N	$-x_N$	R_N	$-x_N$	R_N
6.92	3.500	0.00	2.030	0.00	2.030
6.57	3.495	.50	2.062	.50	2.062
6.23	3.400	1.00	2.150	1.00	2.150
5.88	3.215	1.50	2.275	1.50	2.275
5.54	2.985	2.00	2.435	2.00	2.435
5.19	2.715			2.50	2.295
4.85	2.550			3.00	2.337
4.50	2.390			3.50	2.362
4.16	2.280			4.00	2.380
3.81	2.190			4.50	2.400
3.46	2.135			5.00	2.415
3.11	2.085			5.50	2.425
2.77	2.060			6.00	2.435
2.08	2.035			6.28	2.435
1.40	2.032				
.69	2.030				
.00	2.030				

Figure 2. - Description of five nozzle contours studied. Equation of parabolic afterbody: $R_a = 4.125 - \frac{4.125}{18^2} x_a^2$. (All dimensions in inches).

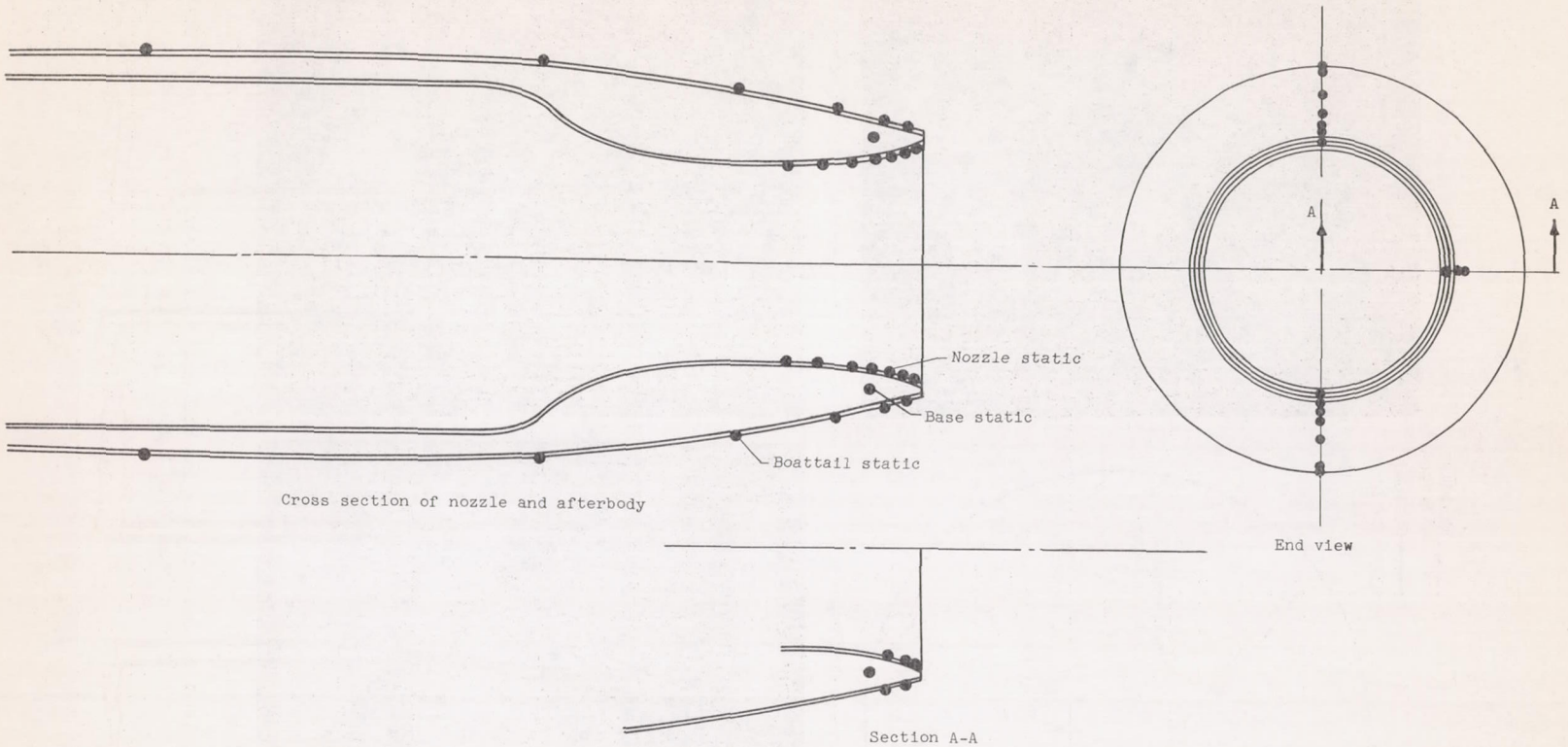

Figure 3. - Location of pressure-measuring orifices on nozzle and afterbody.

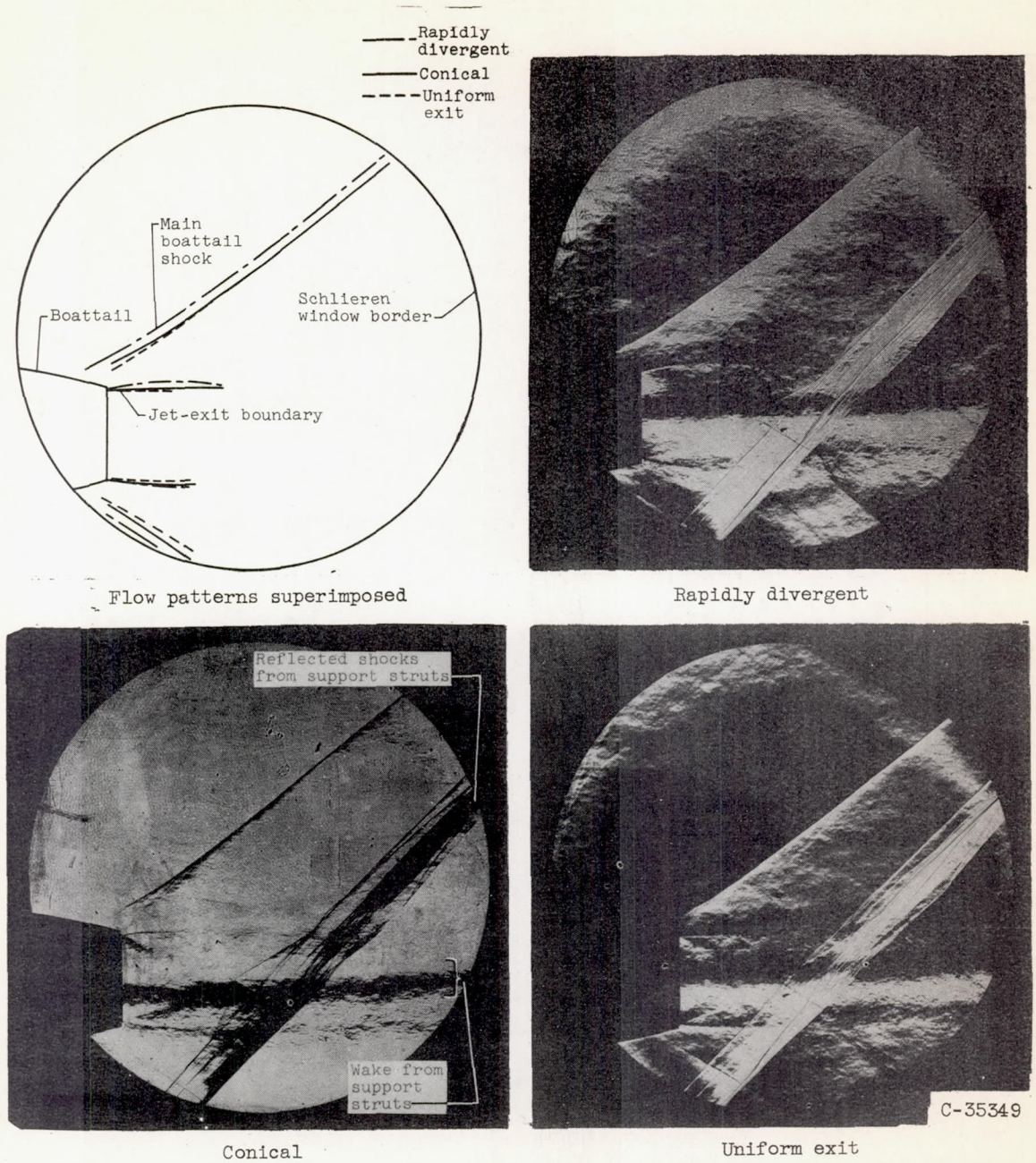

Figure 4. - Comparison of jet-exit angles and boattail-shock positions of convergent-divergent nozzles at free-stream Mach number 1.6 and pressure ratio 8.9.

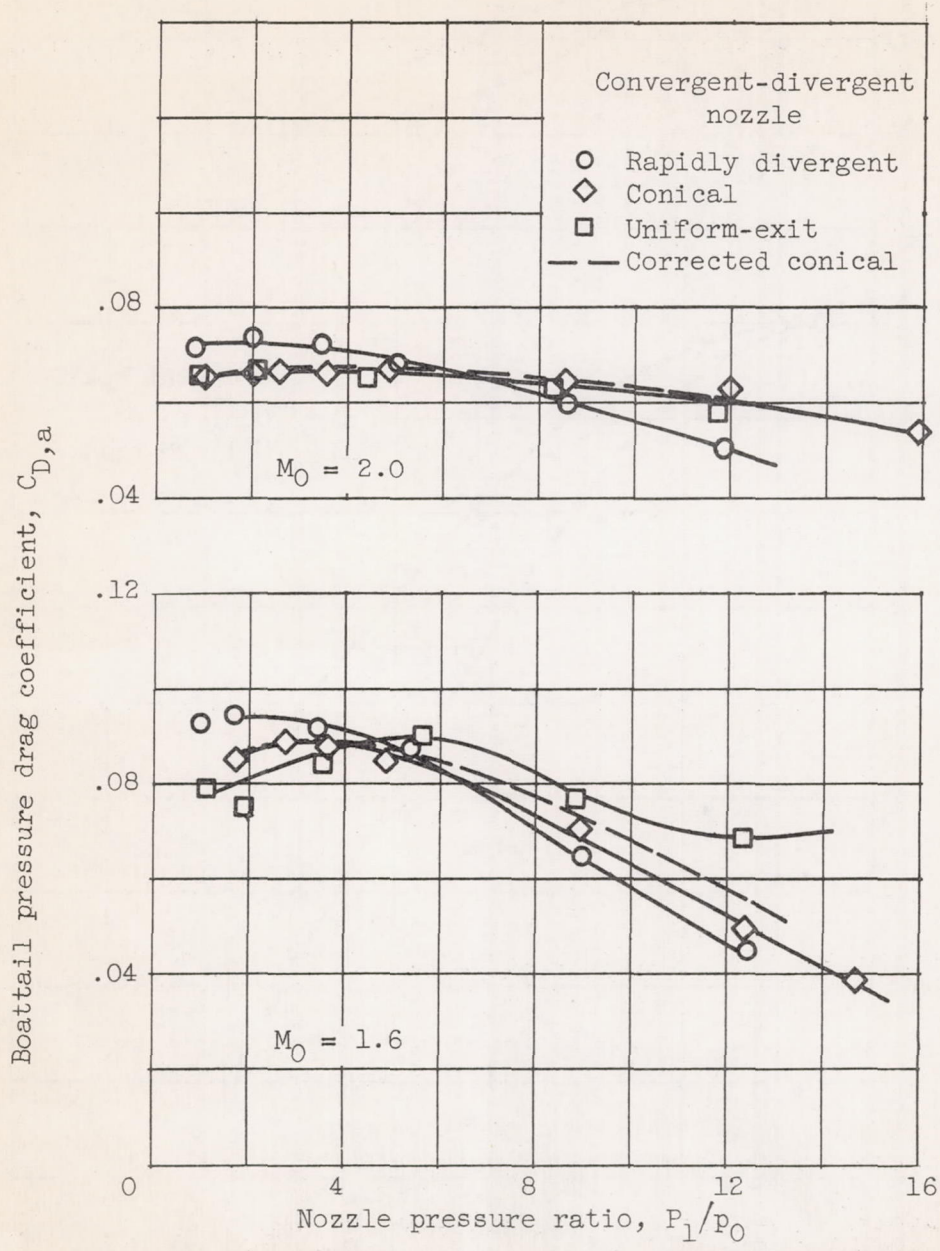

(a) Convergent-divergent nozzles.

Figure 5. - Effect of nozzle contour on boattail pressure drag.

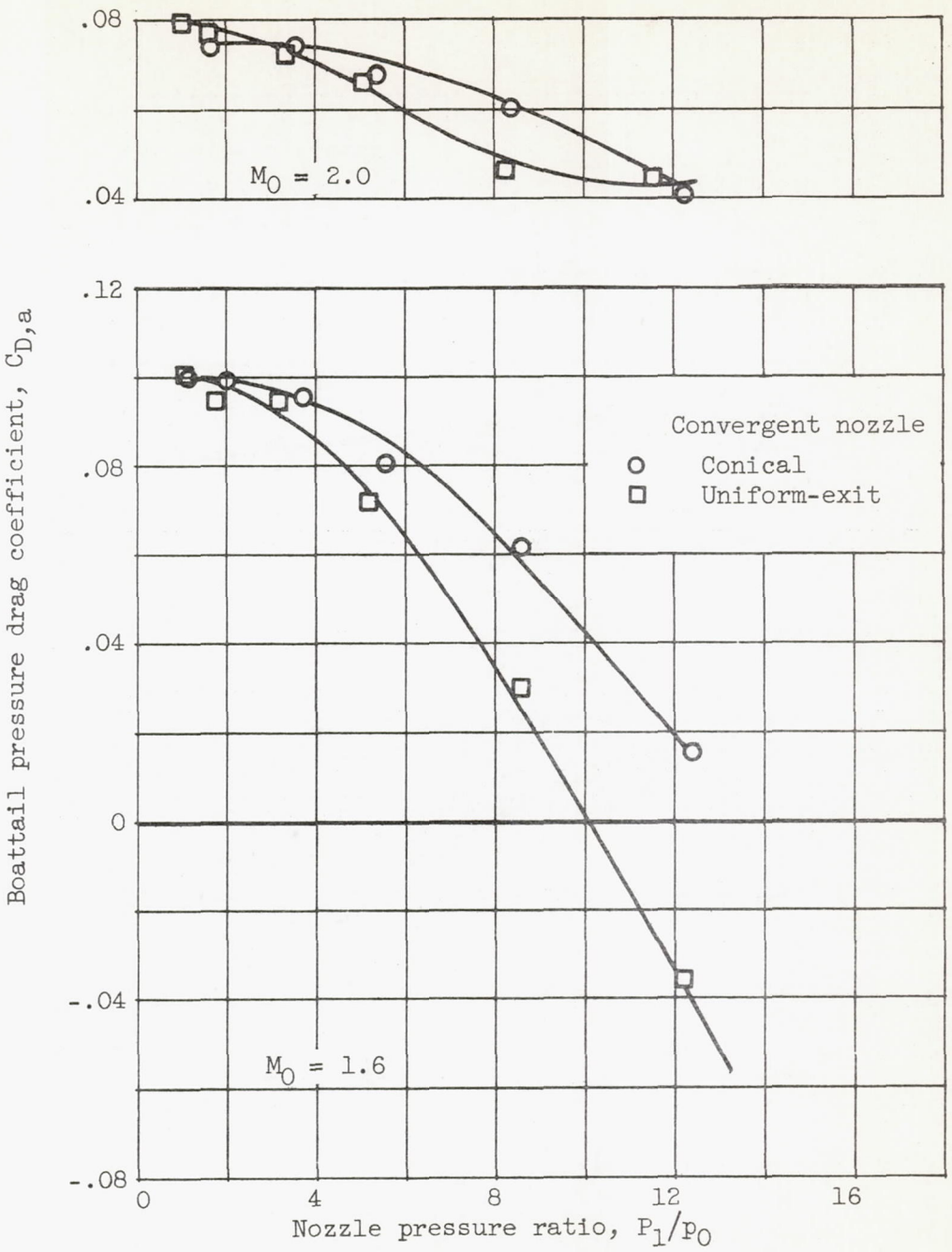

(b) Convergent nozzles.

Figure 5. - Concluded. Effect of nozzle contour on boattail pressure drag.

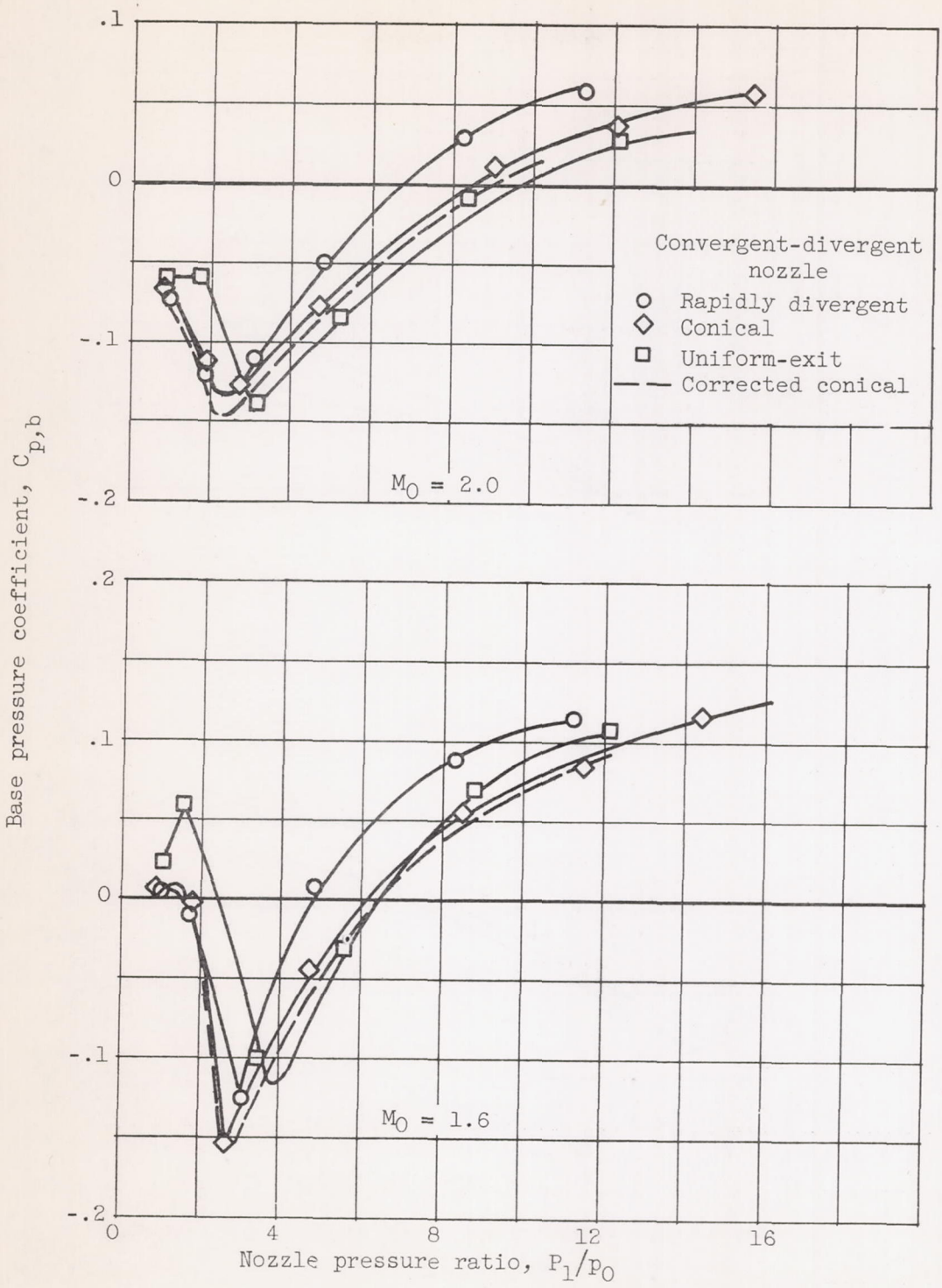

(a) Convergent-divergent nozzles.

Figure 6. - Effect of nozzle contour on base pressure coefficient.

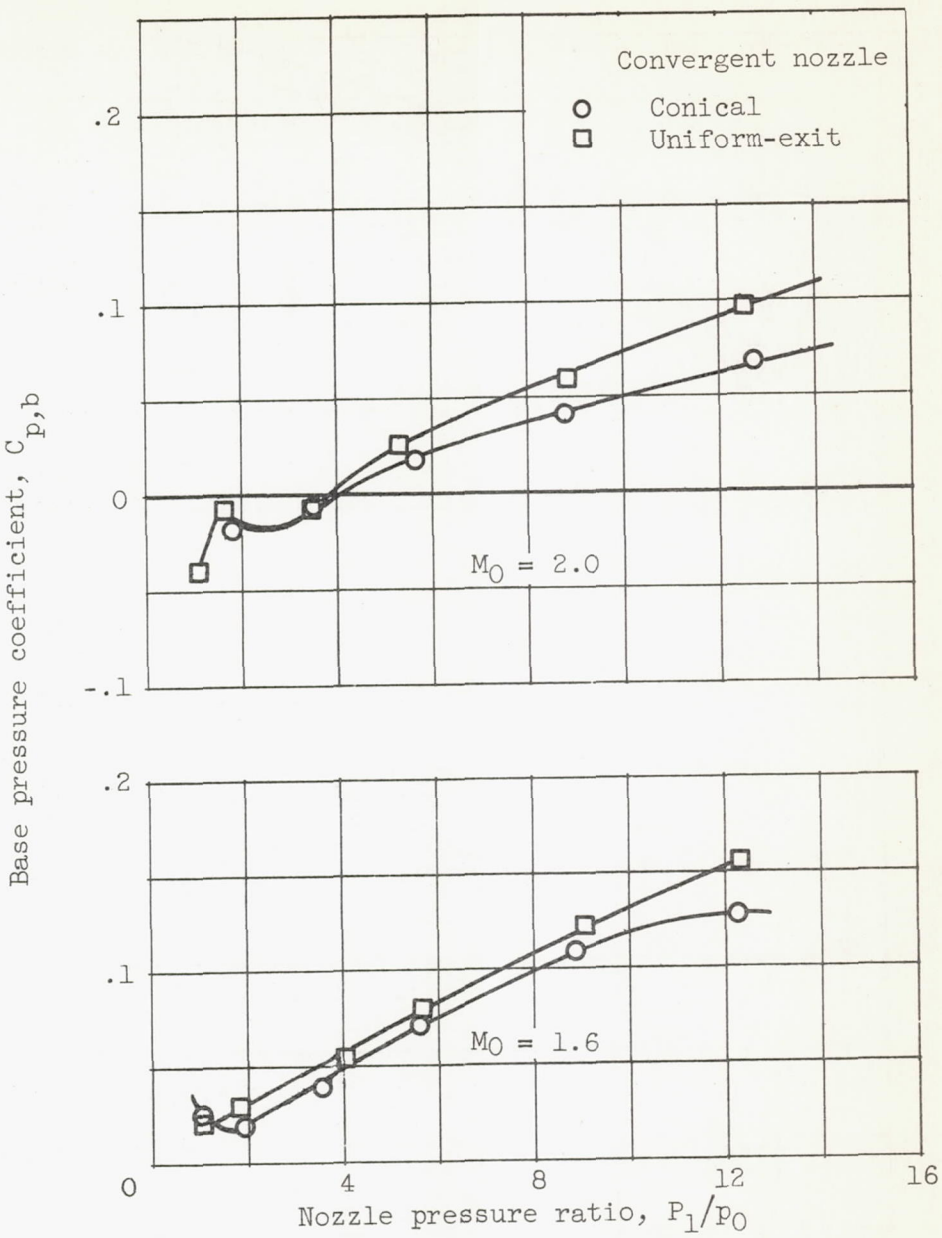

(b) Convergent nozzles.

Figure 6. - Concluded. Effect of nozzle contour on base pressure coefficient.

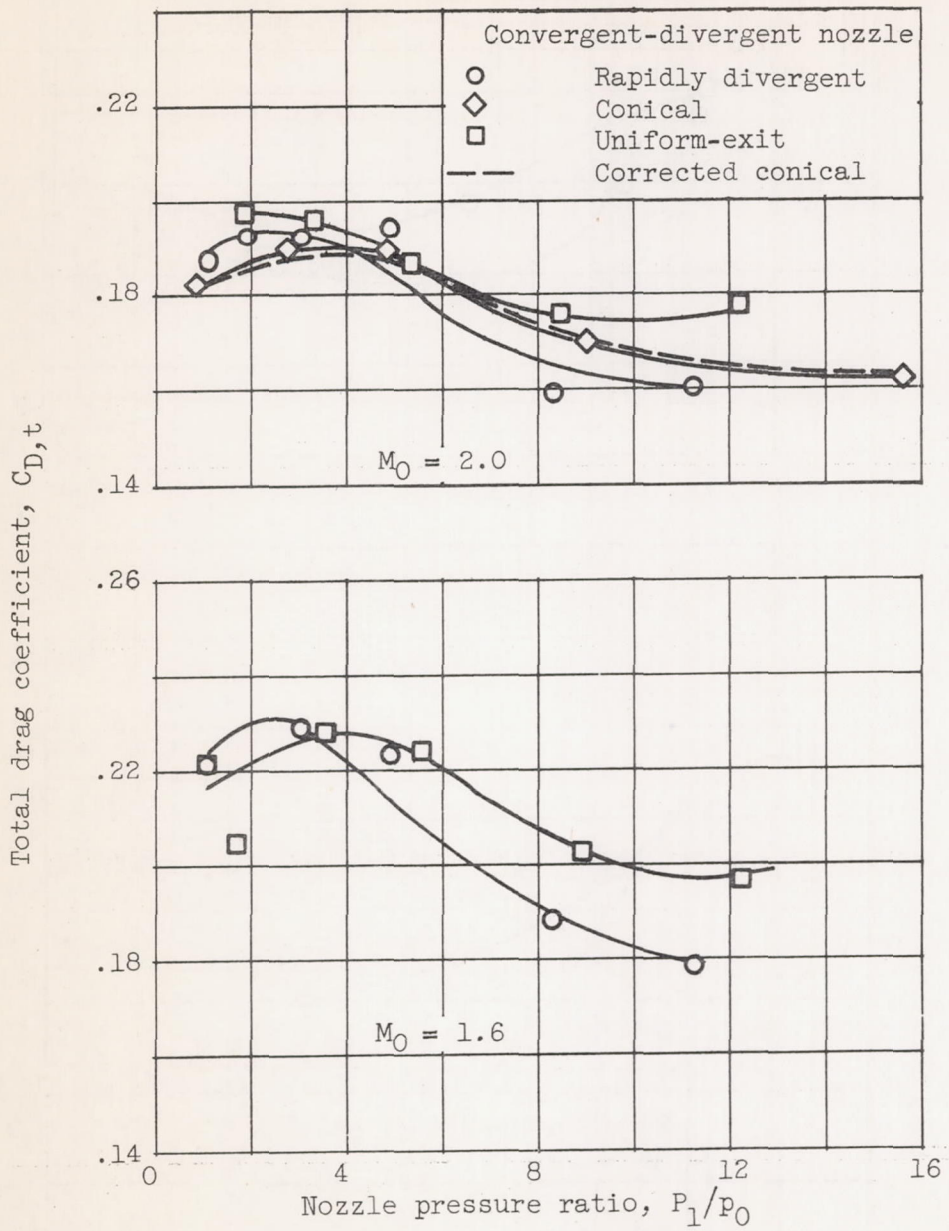

(a) Convergent-divergent nozzles.

Figure 7. - Effect of nozzle contour on total drag.

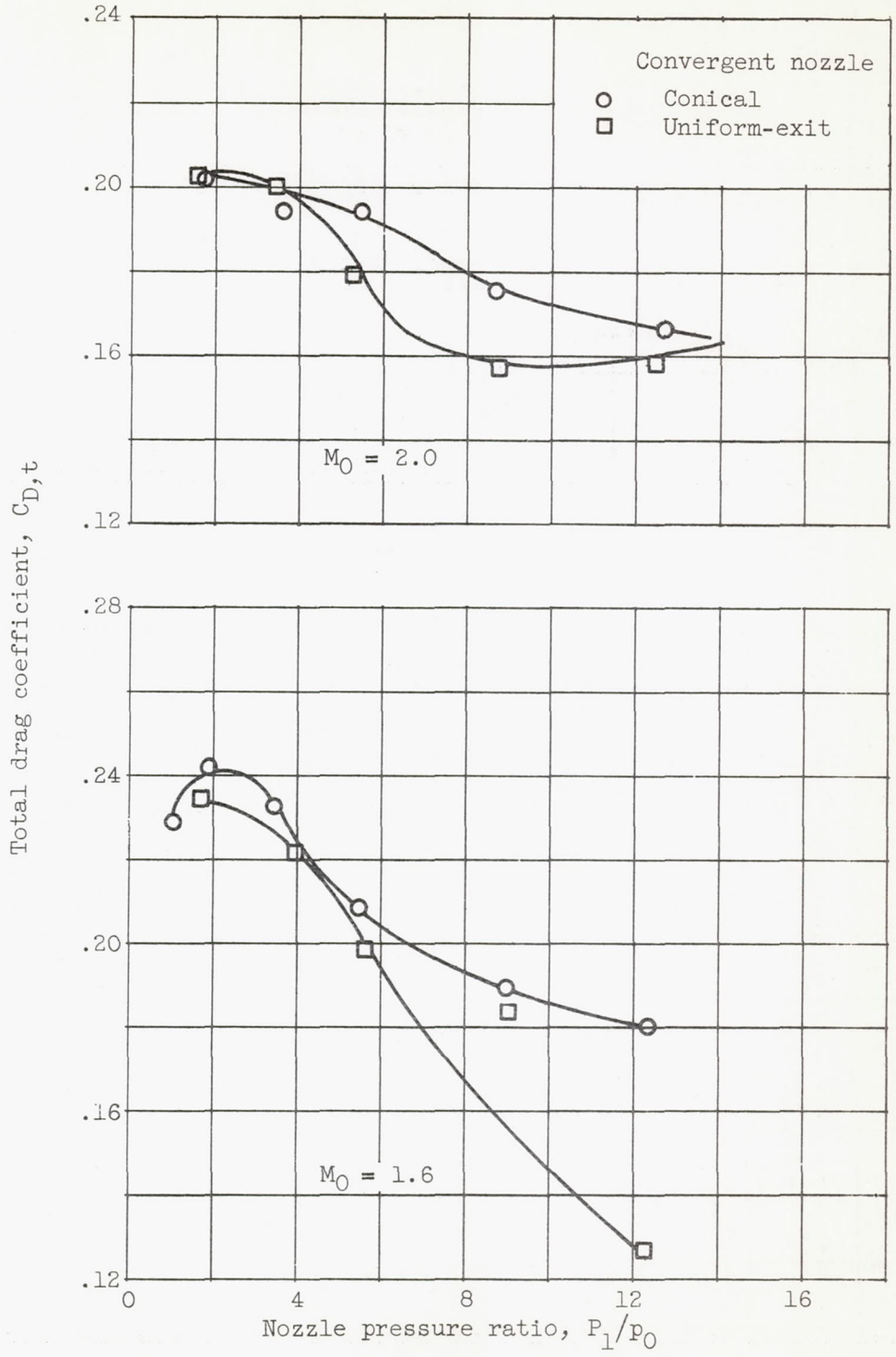

(b) Convergent nozzles.

Figure 7. - Concluded. Effect of nozzle contour on total drag.

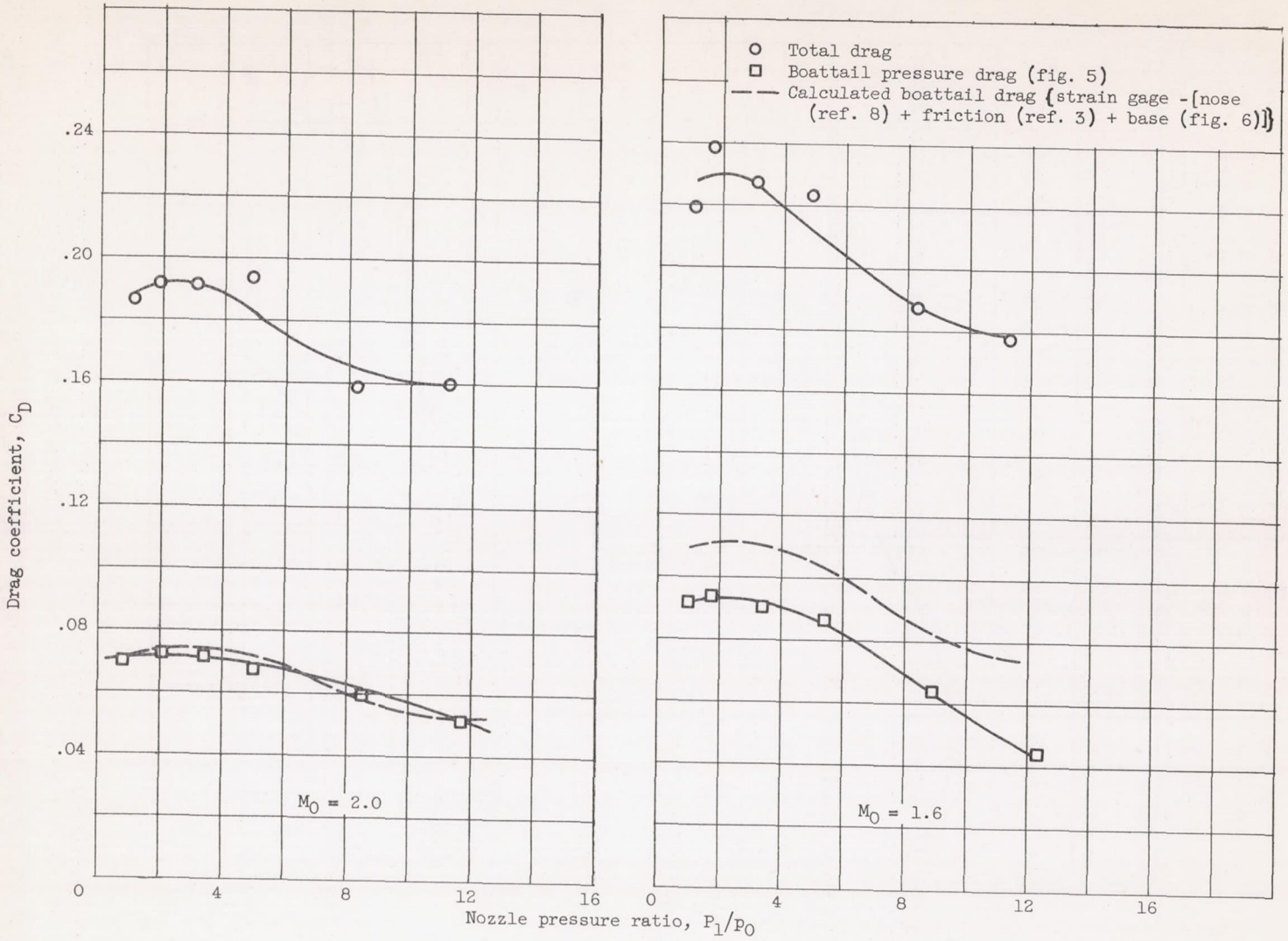

(a) Rapidly divergent nozzle.

Figure 8. - Comparison of boattail pressure drag obtained by two methods.

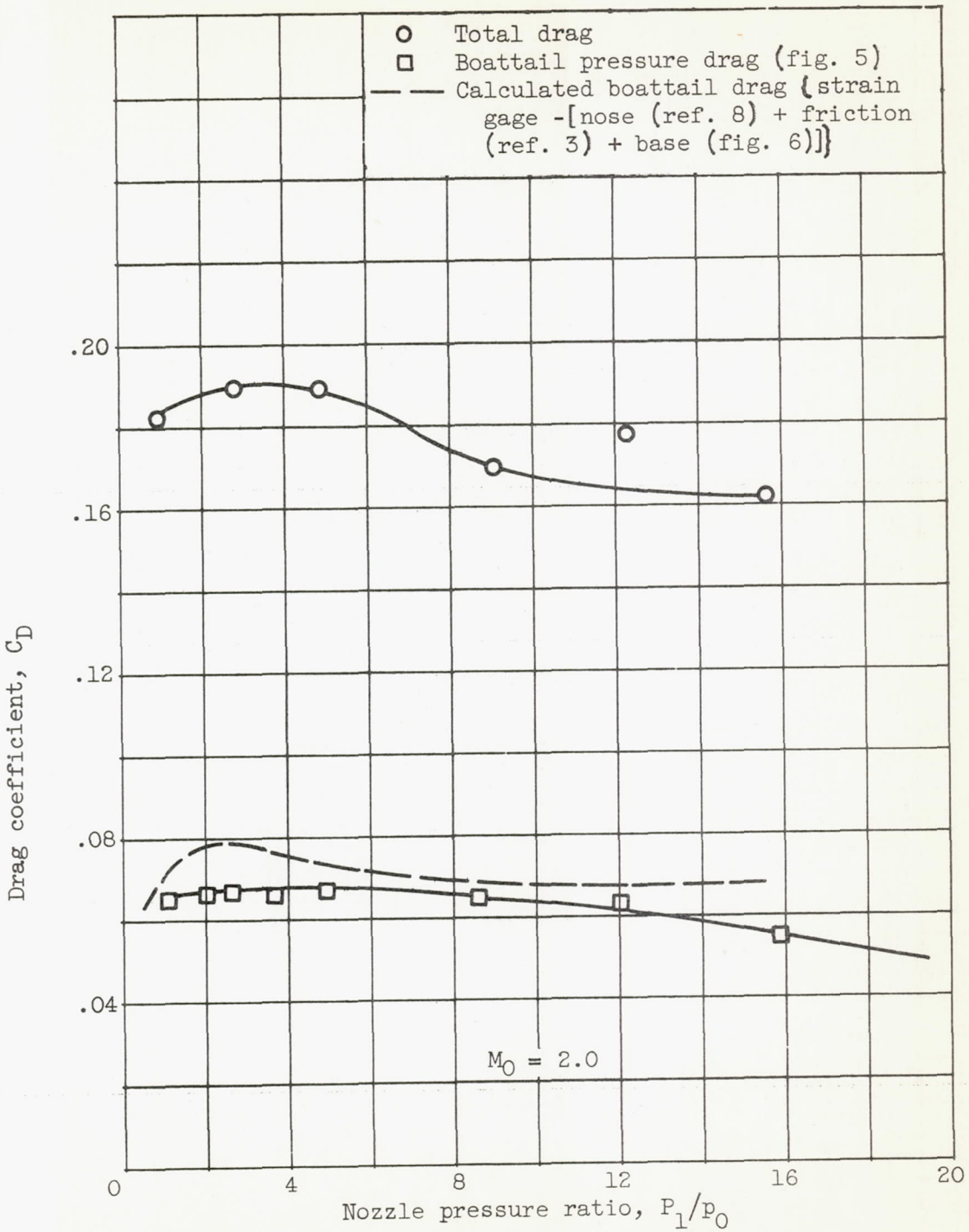

(b) Conical convergent-divergent nozzle.

Figure 8. - Continued. Comparison of boattail pressure drag obtained by two methods.

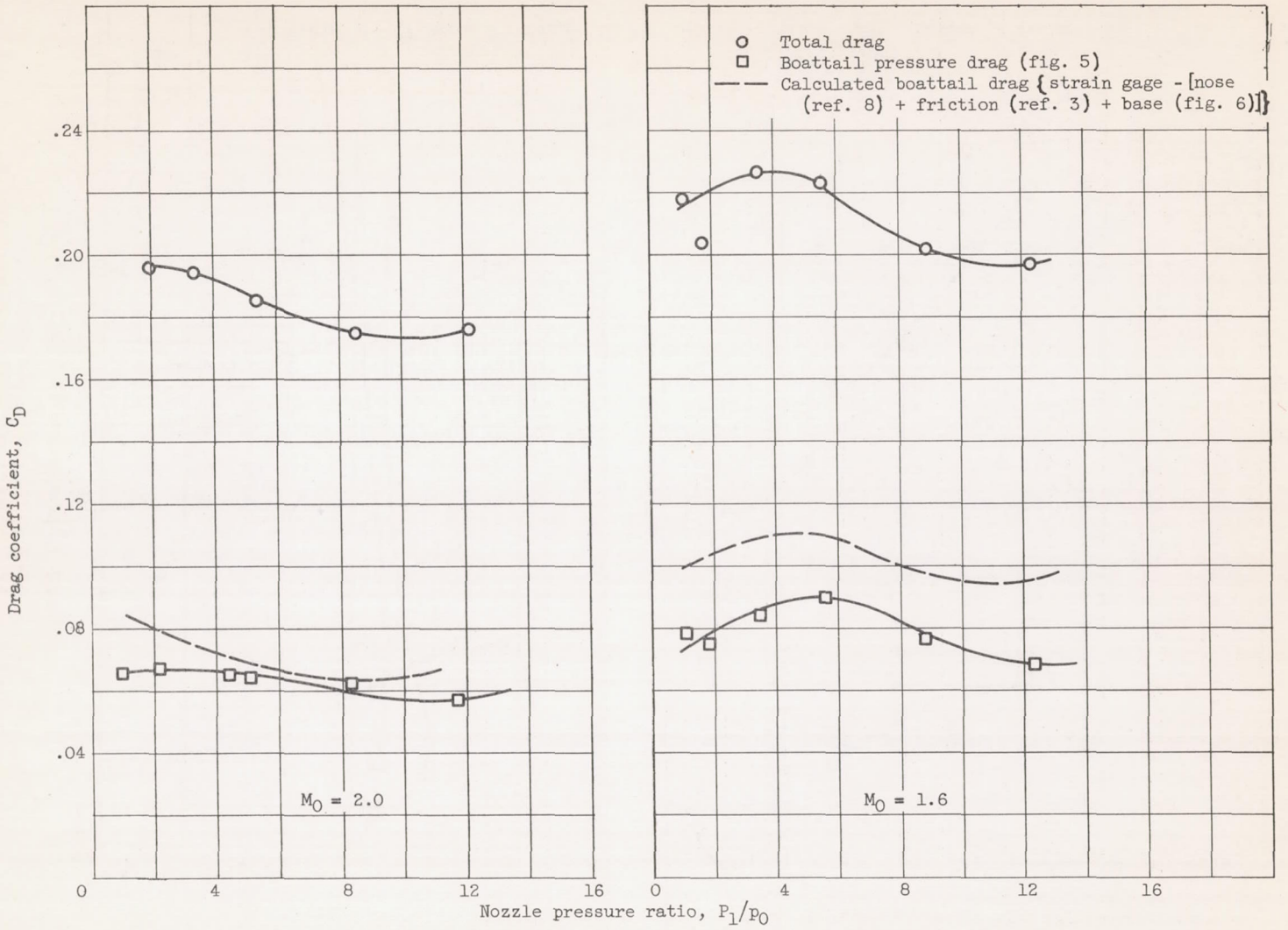

(c) Uniform-exit convergent-divergent nozzle.

Figure 8. - Continued. Comparison of boattail pressure drag obtained by two methods.

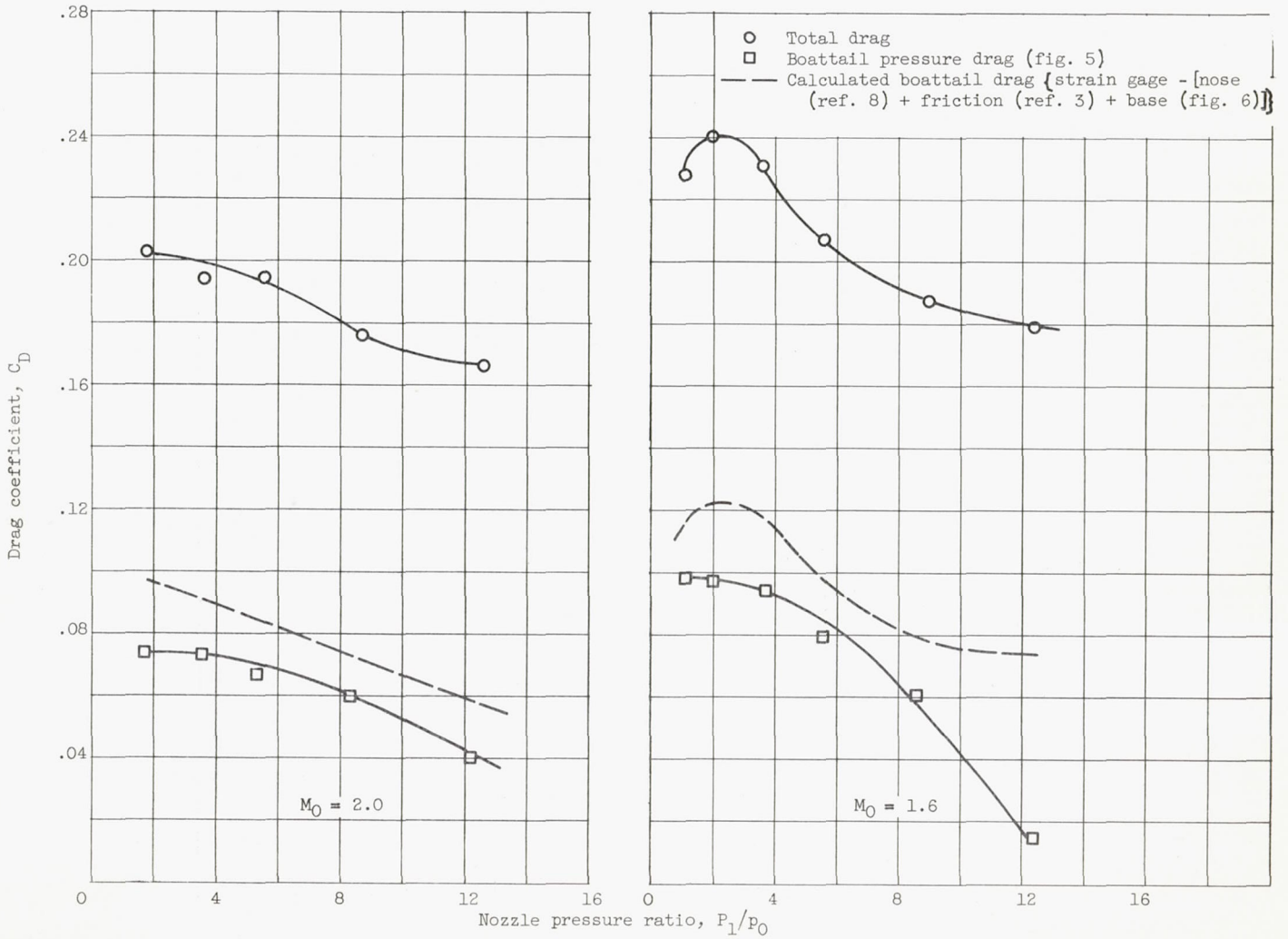

(d) Conical convergent nozzle.

Figure 8. - Continued. Comparison of boattail pressure drag obtained by two methods.

NACA-Langley - 6-21-54 - 350

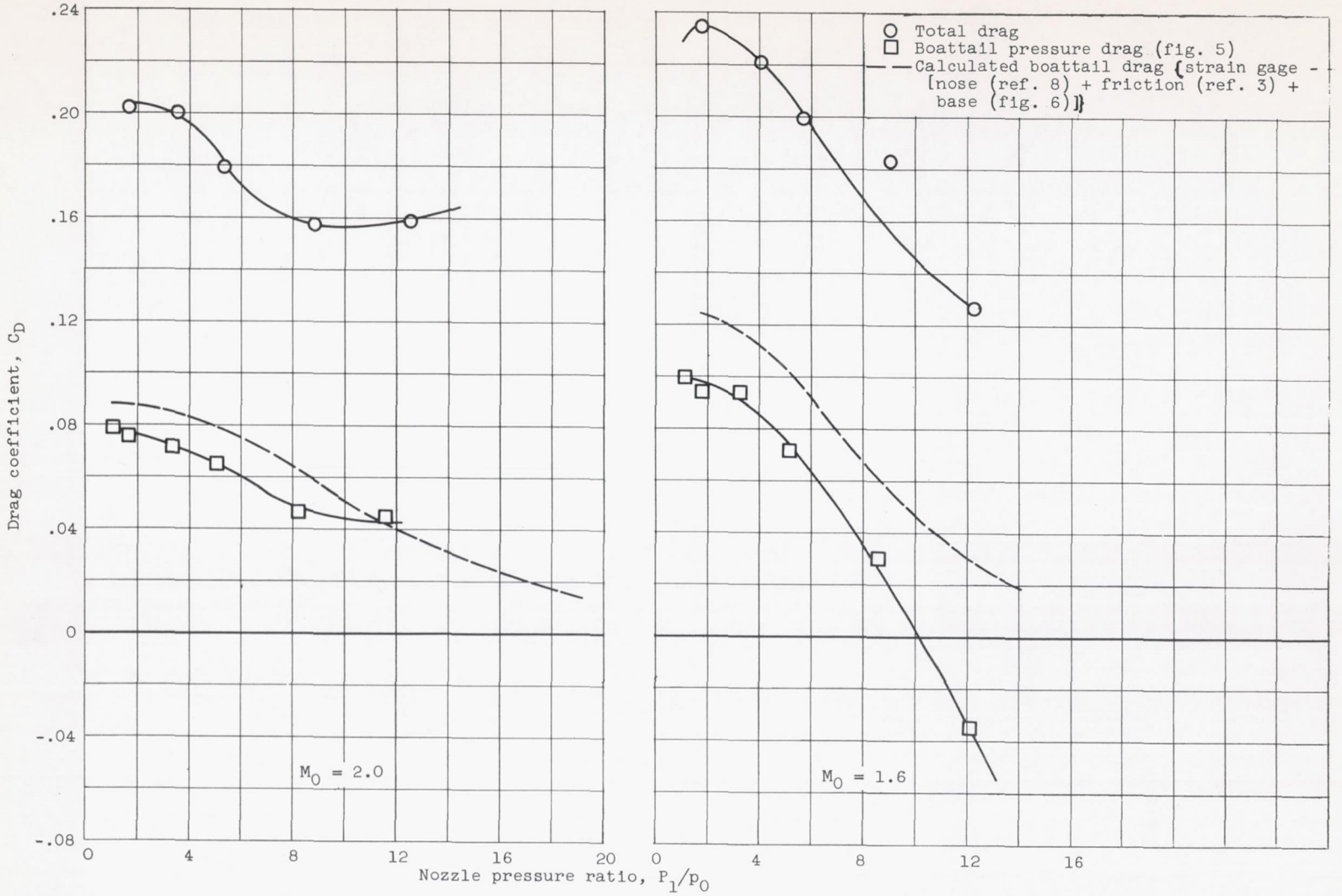

(e) Uniform-exit convergent nozzle.

Figure 8. - Concluded. Comparison of boattail pressure drag obtained by two methods.